JOURNAL OF CATALYSIS **87**, 497–513 (1984)

Mössbauer Emission Studies of Calcined Co–Mo/Al_2O_3 Catalysts: Catalytic Significance of Co Precursors

CARSTEN WIVEL,[1]* BJERNE S. CLAUSEN,† ROBERTO CANDIA,†
STEEN MØRUP,* AND HENRIK TOPSØE[2],†

**Laboratory of Applied Physics II, Technical University of Denmark, DK-2800 Lyngby, Denmark, and*
†Haldor Topsøe Research Laboratories, DK-2800 Lyngby, Denmark

Received March 29, 1983; revised November 9, 1983

The nature of Co in calcined Co–Mo/Al_2O_3 catalysts and the changes that occur upon sulfiding have been investigated by Mössbauer emission spectroscopy (MES). The studies of Co–Mo/Al_2O_3 catalysts show that changes in the Co loading, calcination temperature, and impregnation procedure significantly alter the Co phase distribution. In catalysts with low Co loading, two different types of Co species are generally present: one is identified as tetrahedrally coordinated Co (Co_{tet}) and another is ascribed to cobalt atoms located in octahedral-like coordination (Co_{oct}). The Co_{oct} species, which seem to be located at or close to the surface of the alumina, dominate at low calcination temperatures, whereas calcination at high temperatures favors formation of the Co_{tet} species which appear to be predominantly located in the interior of the alumina. The Co_{tet} species have MES parameters different from those of $CoAl_2O_4$. Catalysts with high Co loadings also contain Co_3O_4. The concentrations of the different Co species in the various calcined Co–Mo/Al_2O_3 catalysts have been compared with the corresponding data for the same catalysts after sulfiding. It is found that the fraction of Co which is present in the alumina after sulfiding is related to the amount of Co_{tet}, the amount of Co_9S_8 is related to Co_3O_4, and Co in the catalytically active Co–Mo–S phase is related to Co_{oct}. As a consequence of the latter, the thiophene hydrodesulfurization activity is related to the amount of Co_{oct} in the calcined catalysts.

INTRODUCTION

Many different locations have been proposed for the Co promoter atoms in calcined Co–Mo/Al_2O_3 hydrodesulfurization (HDS) catalysts (*1–6*). These include interaction with the alumina support, aggregation as a separate oxide phase (CoO or Co_3O_4), and interaction with Mo to form $CoMoO_4$ or a specific Co–Mo surface species.

Mössbauer emission spectroscopy (MES) has been successfully applied for studies of the catalysts (*6–17*), including especially the relevant sulfided state. Coexistence of three phases has been demonstrated, namely, Co inside the alumina structure (Co : Al_2O_3), Co in a Co_9S_8 phase, and Co in a highly dispersed "Co–Mo–S" phase. Co–Mo–S was found to be the most catalytically important phase, since HDS promotion is directly relatable to its Co content (*6, 11, 13–17*).

The activity of sulfided Co–Mo/Al_2O_3 may be related to properties of the calcined (oxidic) state (*3, 6, 11, 17–22*), although there is little agreement on the reasons for this. The proposal of the Co–Mo–S phase appears to have rationalized this. In fact, it was found that NO adsorption, diffuse reflectance spectroscopy (DRS), and magnetic susceptibility results on the calcined state relate to the amount of Co present as Co–Mo–S after sulfiding (*17, 22*).

In order to obtain further insight into the state of Co in calcined catalysts, we have performed detailed MES studies of different calcined Co–Mo/Al_2O_3 catalysts.

---

[1] Present address: Dansk Boreselskab A/S, DK-1263 Copenhagen, Denmark.

[2] To whom correspondence should be addressed.

0021-9517/84 $3.00

METHODS

A. Sample Preparation

The Co–Mo/Al_2O_3 catalysts were prepared by coimpregnation (Co–Mo/Al_2O_3 (coimp)) and by sequential impregnation procedures in which either molybdenum or cobalt was added first. The Co–Mo/Al_2O_3 (coimp) catalysts were prepared by impregnating γ-Al_2O_3 (230 m^2/g) with an ammoniacal solution of cobalt nitrate and ammonium heptamolybdate. The impregnated samples were dried in air at room temperature and afterwards calcined in air for 24 hr at 775 K.

The Co–Mo/Al_2O_3 (Co first) catalyst was prepared by first impregnating the alumina with cobalt nitrate (using the pore filling method) followed by drying at room temperature and calcining at 775 K for 2 hr. This Co/Al_2O_3 catalyst was then impregnated with a solution of ammonium heptamolybdate giving a catalyst with a Co/Mo atomic ratio of 0.8 (5.2 wt% Co and 10.6 wt% Mo). After drying, the catalyst was calcined at 775 K for 2 hr. Numbers in the catalyst notation give the weight percent of the metals. For example, Co1–Mo6/Al_2O_3 signifies that the catalyst contains 1 wt% Co and 6 wt% Mo.

The preparation of the Co–Mo/Al_2O_3 (Mo first) catalysts has been reported in detail earlier (*13*). A Mo/Al_2O_3 (8.6% Mo) catalyst was prepared by impregnating η-Al_2O_3 (250 m^2/g) with an ammoniacal solution of ammonium heptamolybdate followed by drying and by calcining in air at 775 K for 2 hr. The amount of Mo in this catalyst corresponds to less than a monolayer coverage. The Co–Mo/Al_2O_3 catalysts were then prepared by impregnating (using the pore filling method) the above Mo/Al_2O_3 catalysts with aqueous solutions of cobalt nitrate. After drying, the Co–Mo/Al_2O_3 catalysts were calcined in air at 775 K for 2 hr. Catalysts containing only Co (Co/Al_2O_3) were prepared in a similar fashion.

The model compounds, CoO, Co_3O_4, $CoAl_2O_4$, and $CoMoO_4$, were all laboratory synthesized. CoO was prepared by heating cobalt nitrate in a flow of air to 1225 K. After 12 hr at this temperature, the sample was slowly cooled to room temperature in a flow of N_2. XRD measurements showed well-crystallized CoO with no other phases present. Co_3O_4 was prepared from the above CoO sample by heating it in air to 925 K for 72 hr followed by slow cooling to room temperature. X-Ray diffraction (XRD) measurements showed well-crystallized Co_3O_4 with minor amounts (<5%) of CoO. The preparation of $CoAl_2O_4$ was carried out by adding stoichiometric amounts of cobalt nitrate and aluminum nitrate to a citric acid solution and evaporating to dryness at 310 K. The residue was then calcined in air at 820 K for 12 hr. Only well-crystallized $CoAl_2O_4$ could be detected by XRD measurements. α-$CoMoO_4$ was prepared by coprecipitation from boiling solutions of stoichiometric mixtures of cobalt nitrate and sodium molybdate. After thorough washing, the precipitate was calcined in air at 775 K. The identity of the compound was verified by its XRD pattern. In order to study the above samples by MES, radioactive ^{57}Co was added to the cobalt nitrate solutions used in the preparations.

B. Mössbauer Spectroscopy Measurements

In the present MES studies the catalysts and the model compounds were used as stationary sources and spectra were collected using a constant acceleration spectrometer with a moving single line absorber of $K_4[Fe(CN)_6] \cdot 3H_2O$ enriched in ^{57}Fe (*12*). Zero velocity is defined as the centroid of a spectrum obtained at room temperature with a source of ^{57}Co in metallic iron. Positive velocity corresponds to the absorber moving away from the source.

RESULTS

Before presenting the MES results, it may be useful to mention that the MES technique provides information about the Co-containing phases, i.e., we study the

TABLE 1

Mössbauer Emission Spectroscopy Parameters of Model Compounds

Compound	Temp. (K)	Fe^{3+} component(s)		Fe^{2+} component(s)	
		δ (mm s^{-1})	ΔE_Q (mm s^{-1})	δ (mm s^{-1})	ΔE_Q (mm s^{-1})
CoO	570	0.22 ± 0.02	0	0.90 ± 0.02	0
	300	0.39 ± 0.02	0	1.07 ± 0.02	0
Co_3O_4	570	0.14 ± 0.05	0.53 ± 0.05		
		0.08 ± 0.05	0		
	300	0.35 ± 0.03	0.56 ± 0.03		
		0.28 ± 0.03	0		
	80	0.43 ± 0.02	0.54 ± 0.02		
		0.37 ± 0.02	0		
$CoAl_2O_4$[a]	570	0.11 ± 0.05	0.65 ± 0.05	0.61 ± 0.09	0.82 ± 0.09
	300	0.23 ± 0.05	0.61 ± 0.05	0.97 ± 0.09	1.14 ± 0.08
	80	0.23 ± 0.05	0.69 ± 0.05	1.21 ± 0.09	2.35 ± 0.09
$CoMoO_4$	300	0.43 ± 0.04	0.49 ± 0.04	1.06 ± 0.03	1.33 ± 0.03
				1.12 ± 0.07	2.59 ± 0.07
	80	0.45 ± 0.04	0.56 ± 0.04	1.20 ± 0.02	1.71 ± 0.02
				1.26 ± 0.06	2.70 ± 0.06

[a] The spectra have been fitted using only one Fe^{3+} doublet and one Fe^{2+} doublet although the spectra clearly show that a distribution in Mössbauer parameters exists. The values given are therefore only approximate.

^{57}Fe atoms produced by the decay of the ^{57}Co atoms. The decay may give rise to so-called chemical after-effects, i.e., formation of unstable valence and spin states of the daughter atoms. These effects in some instances give rise to an undesirable complication in the interpretation of spectra obtained for Co–Mo/Al_2O_3 catalysts (*10*). However, the after-effects are found to be very sensitive to the local structure and may therefore be used for identifying small changes in the cobalt-containing phase.

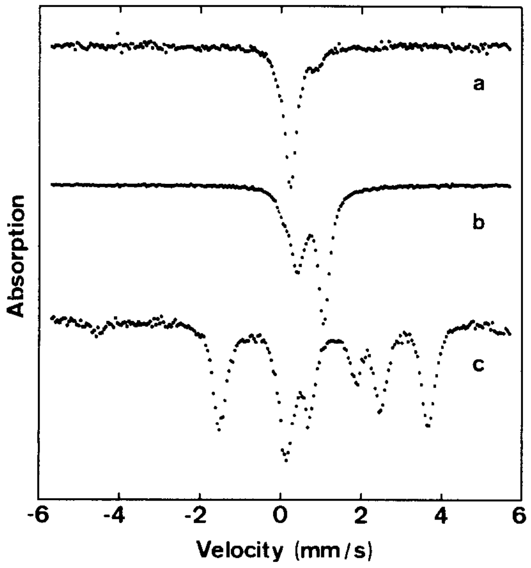

FIG. 1. Mössbauer emission spectra of CoO: (a) 575 K, (b) 300 K, (c) 80 K.

A. Cobalt Model Compounds and Co/Al_2O_3 Catalysts

a. CoO. The MES spectra of CoO recorded at 575, 300, and 80 K are shown in Fig. 1. The Mössbauer parameters (Table 1) agree with those reported previously (*23, 24*). Above the Néel temperature (291 K), the spectra contain a Fe^{2+} and a Fe^{3+} single line component. At high temperatures the Fe^{3+} component dominates. As expected, the values of the isomer shifts for both components are typical of octahedrally coordinated ions since CoO has a NaCl structure above the transition temperature. The spectrum recorded at 80 K shows that both the ferrous and the ferric

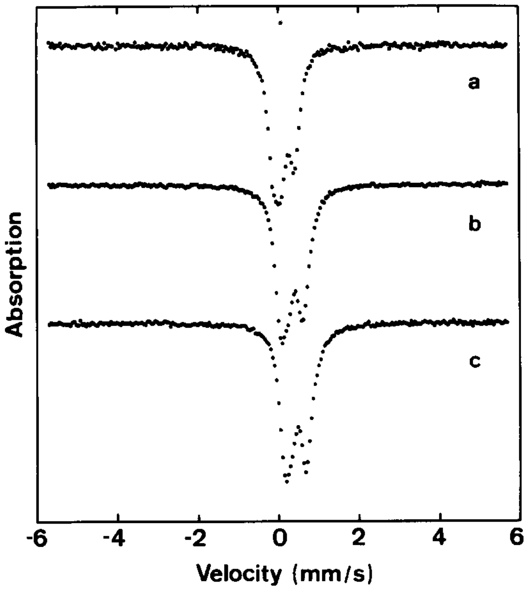

FIG. 2. MES spectra of Co_3O_4: (a) 575 K, (b) 300 K, (c) 80 K.

components in CoO become magnetically split below the Néel temperature.

b. Co_3O_4. Figure 2 shows MES spectra of Co_3O_4 recorded at 575, 300, and 80 K. The spectra are in accordance with those obtained by Spencer and Schroeer (*25*) and can be interpreted in terms of a quadrupole doublet and a single line. Table 1 gives the Mössbauer parameters at room temperature as well as at 575 and 80 K. Co_3O_4 has a normal spinel structure in which the symmetry of the tetrahedral sites is cubic, whereas this is not the case for the octahedral sites. Thus, the doublet originates from the octahedral ions, whereas the single line is due to the tetrahedral ions. The values of the isomer shifts and the area ratio of the two components corroborate this assignment. The results also show that in this compound both the tetrahedral Co^{2+} and the octahedral Co^{3+} ions decay to trivalent iron ions.

c. $CoAl_2O_4$. MES spectra of $CoAl_2O_4$ recorded at 575, 300, and 80 K are shown in Fig. 3. These spectra all show the presence of two quadrupole doublets, one arising from Fe^{3+} and the other from Fe^{2+}. The isomer shifts of both components are relatively low (Table 1) being typical of tetrahedrally coordinated ions. This is in accordance with the structure of $CoAl_2O_4$ in which the Co ions predominantly occupy tetrahedral sites. It is seen that both Fe^{2+} and Fe^{3+} ions are produced by the decay of the Co^{2+} ions. This behavior is similar to that observed for CoO and has also been found for other cobalt-containing spinels (*25*). The lines due to the Fe^{2+} ions are broad and asymmetric indicating that a distribution of local surroundings exists. This is probably related to the fact that $CoAl_2O_4$ is not a completely normal spinel, i.e., the structure has a small fraction of Co^{2+} ions in octahedral environments (see, e.g., Ref. (*26*)).

d. $CoMoO_4$. MES spectra of the low-temperature form (the so-called α-form) of $CoMoO_4$ have previously been discussed by Clausen *et al.* (*27*). Spectra recorded at 300 and 80 K are shown in Fig. 4. The room temperature spectrum can be analyzed in terms of one Fe^{3+} quadrupole doublet and two Fe^{2+} quadrupole doublets with the Mössbauer parameters listed in Table 1.

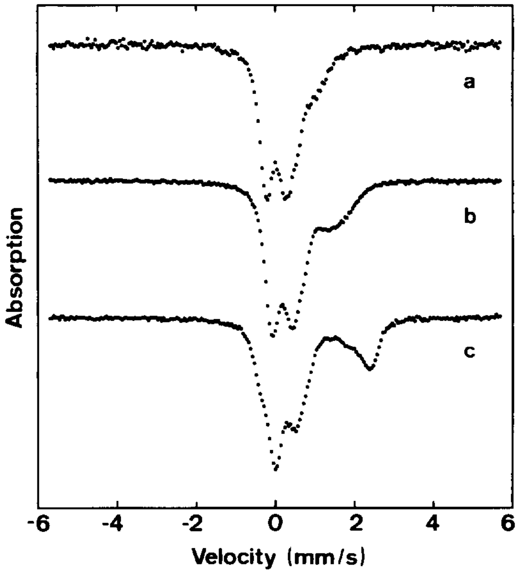

FIG. 3. MES spectra of $CoAl_2O_4$: (a) 575 K, (b) 300 K, (c) 80 K.

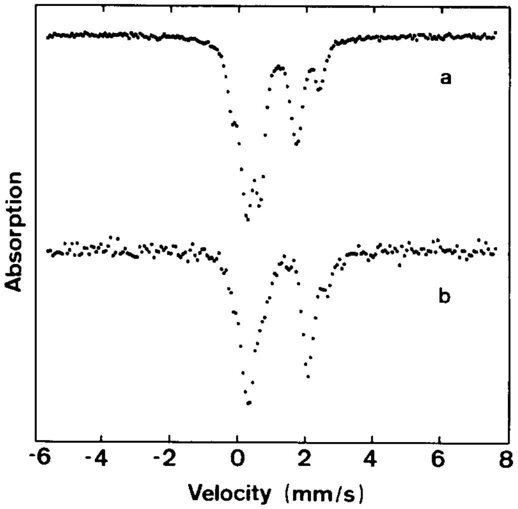

FIG. 4. MES spectra of α-$CoMoO_4$: (a) 300 K, (b) 80 K.

Thus, Fe^{3+}, as well as Fe^{2+}, are present after the decay of Co^{2+}. As in CoO, the Fe^{3+}/Fe^{2+} ratio decreases as the temperature is lowered. The presence of two Fe^{2+} quadrupole doublets is in accordance with the crystal structure of $CoMoO_4$ in which the Co atoms occupy two crystallographically different sites (*28*). The relatively high values of the isomer shifts are also in accordance with the fact that both Co sites in $CoMoO_4$ have (distorted) octahedral symmetry.

e. Co/Al_2O_3 catalysts. Figure 5 shows the MES spectra of the Co 0.25/Al_2O_3, Co 1/Al_2O_3, and Co 5/Al_2O_3 catalysts in the calcined and sulfided states. The spectra of the two catalysts with the lowest Co loadings have quite broad lines. This indicates that the Co atoms in these samples are not present in a well-defined phase but rather in slightly different sites presumably in the alumina. The spectrum of the Co 0.25/Al_2O_3 catalyst is dominated by a ferrous doublet with an isomer shift, $\delta = 1.09 \pm 0.05$ mm/s, and a quadrupole splitting, $\Delta E_Q = 2.13 \pm$

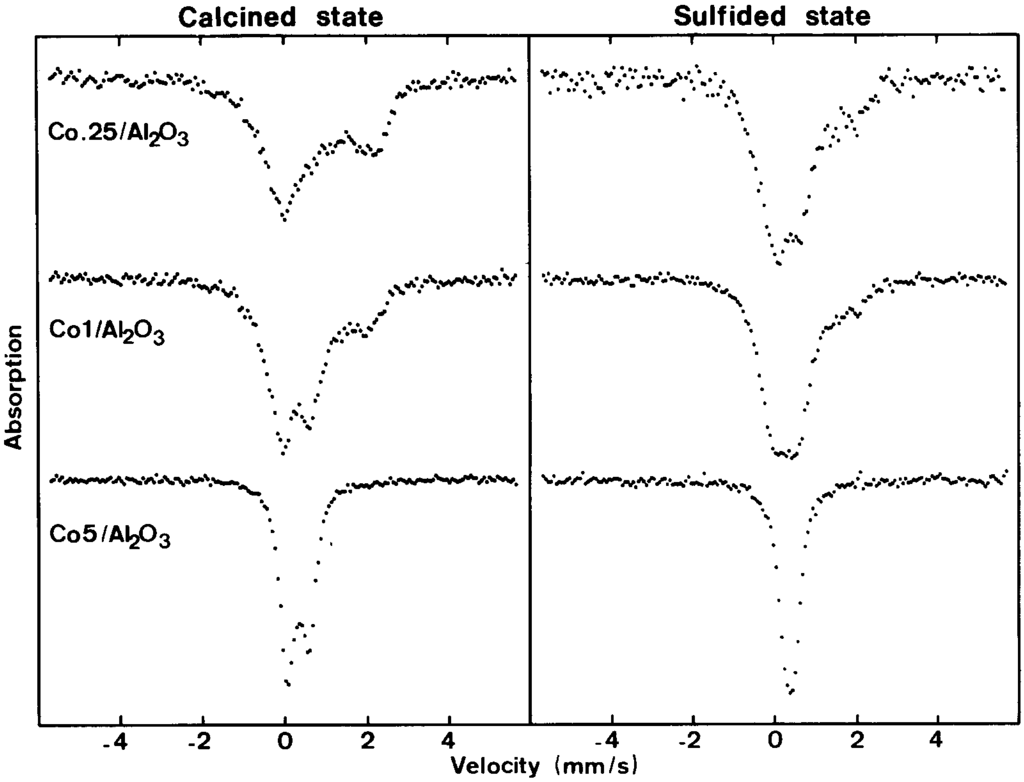

FIG. 5. Room-temperature MES spectra of Co/Al_2O_3 catalysts in the calcined state and in the sulfided state.

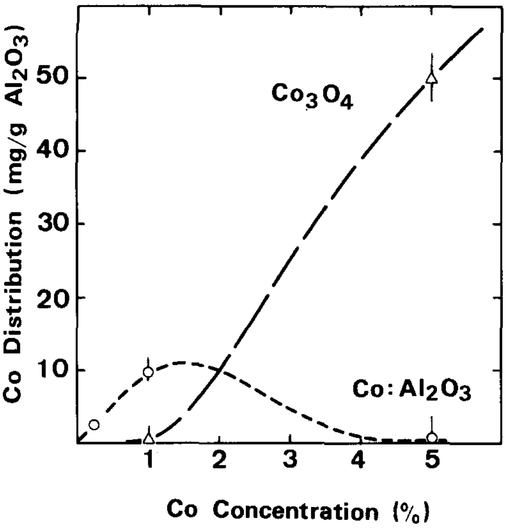

FIG. 6. Absolute amounts of cobalt in Co:Al_2O_3 and Co_3O_4 as a function of the content of Co in the calcined Co/Al_2O_3 catalysts.

0.05 mm/s. A ferric component is also present with the parameters $\delta = 0.39 \pm 0.10$ mm/s and $\Delta E_Q = 0.80 \pm 0.10$ mm/s. The isomer shifts are typical of octahedral coordination. For the catalyst with the highest loading, the Mössbauer lines are narrow in both the calcined and the sulfided state. This indicates that the Co atoms are present in well-defined surroundings. For the calcined state, two components are present with the parameters, $\delta = 0.32 \pm 0.03$ mm/s, $\Delta E_Q = 0.57 \pm 0.03$ mm/s and $\delta = 0.24 \pm 0.03$ mm/s, $\Delta E_Q = 0$ mm/s. From a comparison of these values with those of Co_3O_4 (Table 1), it is found that in the calcined state Co is present as Co_3O_4. XRD measurements confirmed this assignment.

Figure 6 shows the concentration of cobalt in the two different forms as a function of the cobalt loading. It is observed that the concentration of Co associated with the alumina decreases when Co_3O_4 is formed and in the Co 5/Al_2O_3 catalyst it was not possible to detect this phase. After sulfidation of the Co 5/Al_2O_3 catalyst the Mössbauer parameters ($\delta = 0.35 \pm 0.03$ mm/s, $\Delta E_Q = 0.26 \pm 0.03$ mm/s and $\delta = 0.38 \pm 0.03$ mm/s, $\Delta E_Q = 0$ mm/s) show that Co_9S_8 is the dominant cobalt phase present in the catalyst (*12*, *29*). Thus, Co_3O_4 is transformed into Co_9S_8 upon sulfiding.

For the two low-loading catalysts (Co 0.25/Al_2O_3 and Co 1/Al_2O_3) the sulfiding is also observed to affect the local surroundings of the Co atoms (Fig. 5). However, the lines are still broad and Co_9S_8 does not seem to form in any appreciable amount. Also mild oxidation was found to essentially restore the original spectra (*9*).

B. Co–Mo/Al_2O_3 Catalysts

a. Catalysts calcined at different temperatures. Previously, Mössbauer spectra of catalysts calcined at temperatures between 625 and 975 K have been presented (*17*), but no detailed analysis of these spectra was given. Below a more detailed analysis of the spectra, as well as spectra of catalysts calcined at temperatures up to 1125 K, will be given. Figure 7 shows room temperature Mössbauer spectra of Co–Mo/Al_2O_3 (Mo first) catalysts calcined at different temperatures. For comparison, a bar diagram, which indicates the line positions of $CoAl_2O_4$, is inserted. The spectra of the catalysts calcined at 625 K (spectrum a) and 775 K (spectrum b) both show the presence of a ferric doublet and ferrous doublet. It is observed that the lines of both doublets are very broad and the line positions do not coincide with those of $CoAl_2O_4$. The room temperature spectra of the catalysts calcined at 1025 K (spectrum c) and 1125 K (spectrum d) show that with increasing calcination temperatures the spectra of the catalysts become more similar to that of $CoAl_2O_4$. This is easily seen by following, e.g., the change in the line position of the right-hand peak of the ferrous doublet with calcination temperature. Although the room temperature spectra (c) and (d) in Fig. 7 closely resemble that of $CoAl_2O_4$ (Fig. 3b), the temperature dependence of the spectra, illustrated in Fig. 8, is very different from that of $CoAl_2O_4$ (Fig. 3). Thus, the local surroundings of the Co atoms in the catalysts

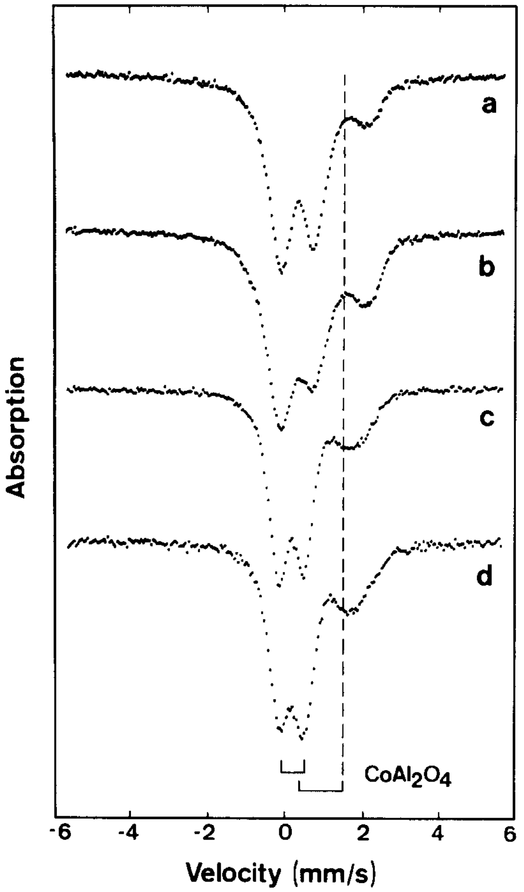

FIG. 7. Room-temperature MES spectra of Co-Mo/Al_2O_3 catalysts calcined at different temperatures: (a) T_{calc} = 625 K, (b) T_{calc} = 775 K, (c) T_{calc} = 1025 K, (d) T_{calc} = 1125 K. The Mössbauer line positions of $CoAl_2O_4$ are indicated by the inserted bar diagram.

and in $CoAl_2O_4$ are different at least for calcination temperatures up to 1125 K.

The spectra of the catalysts calcined at different temperatures were computer fitted using one ferric and one ferrous doublet. Figures 9A and B show the isomer shift and the quadrupole splitting as a function of calcination temperature for the ferrous doublet. It is seen that the isomer shift has a relatively high value when the calcination temperature is less than about 775 K indicating that Co is octahedrally coordinated to oxygen. The analysis shows that also Fe^{3+} in these catalysts is octahedrally coordinated. Calcination temperatures above 775 K result in a decrease in the isomer shift above 775 K (Fig. 9A) and above ca. 975 K it reaches a value typical of Co in tetrahedral coordination. After sulfiding, all the catalysts have a value of the ferrous isomer shift which is essentially identical to that observed for the high temperature calcined catalysts (i.e., typical of Co in tetrahedral coordination). An analysis of the quadrupole splitting (Fig. 9B) shows that the ferrous doublet in the sulfided catalysts resembles that of the ferrous doublet in the catalyst calcined at high temperature (~975 K).

An increase in the calcination temperature from 975 to 1175 K does not significantly alter the value of the isomer shift, whereas the quadrupole splitting decreases but the value which is observed for $CoAl_2O_4$ is not reached. Thus, although Co appears to be predominantly tetrahedrally coordinated in catalysts calcined above ca. 900 K, formation of appreciable amounts of the stoichiometric $CoAl_2O_4$ phase does

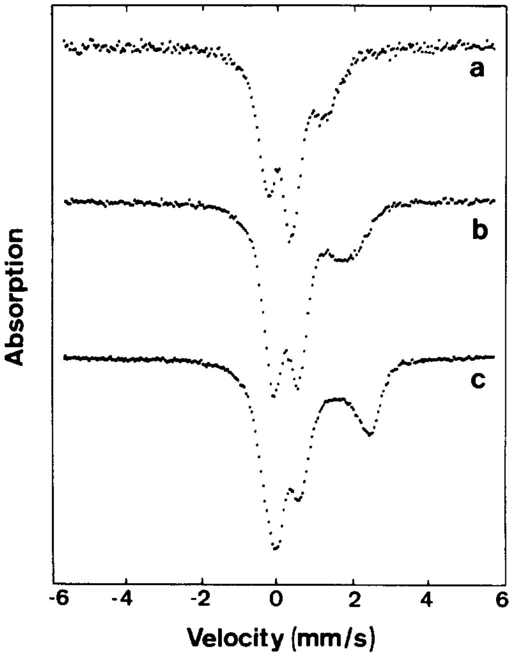

FIG. 8. MES spectra of the Co-Mo/Al_2O_3 catalyst calcined at 1025 K: spectrum at (a) 625 K, (b) 300 K, and (c) 80 K.

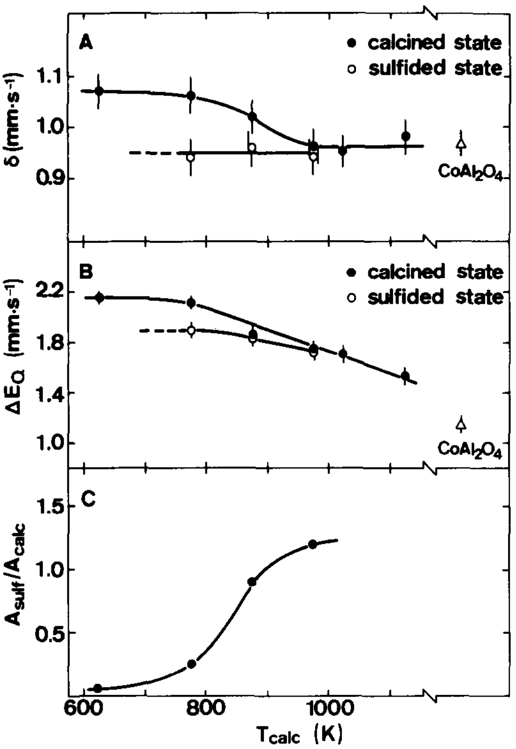

FIG. 9. Room-temperature Mössbauer parameters of the Co–Mo/Al_2O_3 catalysts calcined at different temperatures as a function of T_{calc}. For comparison the values for $CoAl_2O_4$ are inserted.

not occur at the calcination temperatures applied in this study.

The relative area of the ferrous doublet changes upon sulfiding, the extent depending on the prior calcination temperature. This is seen from Fig. 9C where the area ratio of the ferrous doublet after sulfidation to that which existed before sulfiding, A_{sulf}/A_{calc}, is plotted against the calcination temperature. At low calcination temperatures almost all of the ferrous components "disappear" upon sulfiding, whereas a large ferrous component is still present in the spectra of the sulfided catalysts calcined at high temperatures. Although a detailed interpretation is complicated, the results (Fig. 9c) show that the amount of cobalt which can be sulfided decreases with increasing calcination temperature. The observation that A_{sulf}/A_{calc} is actually above 1 for the catalyst calcined at 975 K demonstrates that other factors influence the spectral areas, e.g., minor differences in the local surroundings of the Co atoms may result in small changes in the after-effects (i.e., Fe^{2+}/Fe^{3+} ratio).

b. Catalysts with different Co/Mo ratios. Figure 10 shows spectra of a series of calcined Co–Mo/Al_2O_3 (Mo first) catalysts with different cobalt loadings. These catalysts were all calcined at 775 K. The spectra of the two catalysts with Co/Mo = 0.09 and Co/Mo = 0.27 are quite similar. From the results discussed above it is expected that both Co_{oct} and Co_{tet} species will be present but with Co_{oct} dominating. This is confirmed by a simple analysis of the spectra in terms of only one set of doublets (i.e., one Fe^{2+} and one Fe^{3+} doublet) since this analysis gives parameters (Table 2) typical of octahedral coordination. Upon increasing the Co loading a new spectral component is observed and for the highest loading catalyst this component dominates. A comparison of the spectra of the Co/Mo = 1.9 catalyst with those of Co_3O_4 (Fig. 2) shows that this new component is Co_3O_4.

It is evident that fitting the spectra in terms of only one Fe^{2+} and one Fe^{3+} component is an oversimplification and may only provide information about the predominant Co species. Since the lines are very much broader than the natural linewidth, one should in fact ideally analyze the spectra as consisting of a sum of many components each having lines of natural width. However, such an analysis is questionable when different components have overlapping lines and it is also difficult because the various deconvolution methods available (*30–32*) make assumptions (e.g., that a correlation between the isomer shift and the quadrupole splitting exists), which apply only in special cases. We have therefore used a different approach which simply involves an analysis of the spectra in terms of two sets of components, namely, a Fe^{2+} and a Fe^{3+} component belonging to Co_{oct} and another set consisting of a Fe^{2+} and a Fe^{3+} component belonging to Co_{tet}. The above analysis was carried out using the

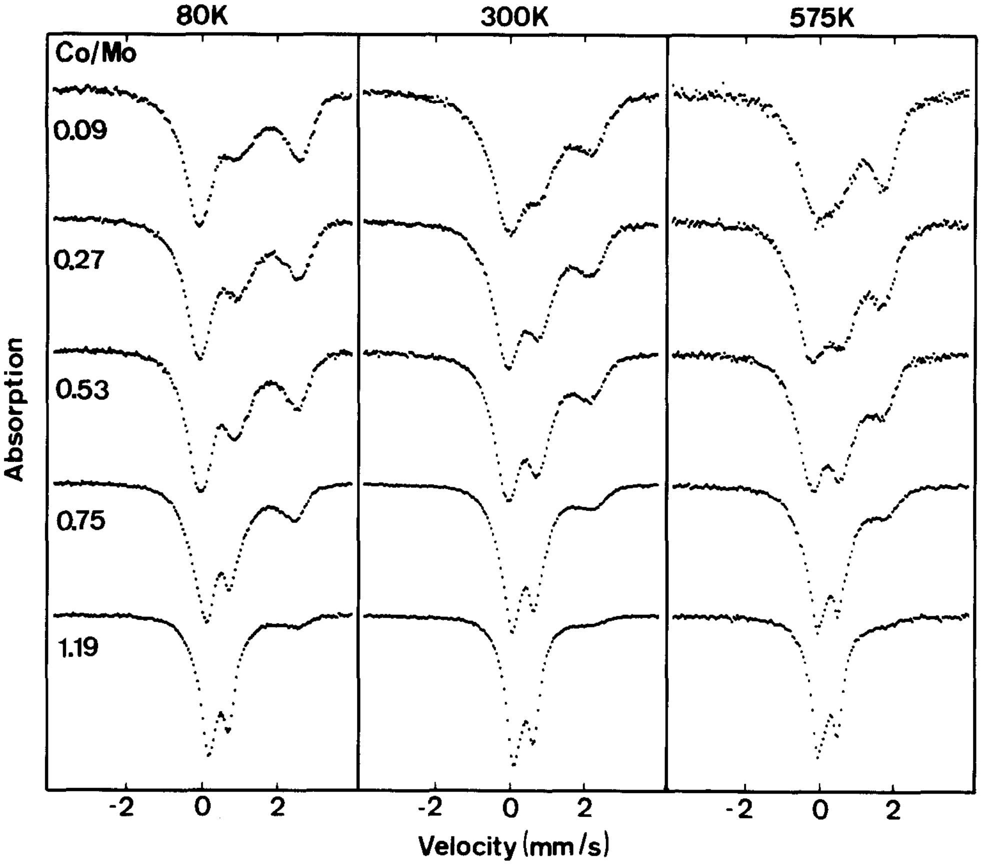

FIG. 10. MES spectra of Co-Mo/Al_2O_3 catalysts with different Co/Mo ratios. The spectra were obtained at 575, 300, and 80 K.

TABLE 2

Mössbauer Emission Parameters for Different Calcined Co-Mo/Al_2O_3 Catalysts

Catalyst	Co/Mo	Temp. (K)	Fe^{3+} component(s)		Fe^{2+} component(s)	
			δ (mm s^{-1})	ΔE_Q (mm s^{-1})	δ (mm s^{-1})	ΔE_Q (mm s^{-1})
Co 0.5–Mo 8.6/Al_2O_3 (Mo first)	0.09	575	0.16 ± 0.09	0.93 ± 0.09	0.88 ± 0.05	1.58 ± 0.05
		300	0.34 ± 0.05	0.94 ± 0.05	1.05 ± 0.05	2.17 ± 0.05
		80	0.42 ± 0.05	1.15 ± 0.09	1.23 ± 0.09	2.60 ± 0.09
Co 1.4–Mo 8.6/Al_2O_3 (Mo first)	0.27	575	0.13 ± 0.09	1.03 ± 0.09	0.83 ± 0.05	1.59 ± 0.05
		300	0.33 ± 0.05	0.96 ± 0.05	1.06 ± 0.05	2.12 ± 0.05
		80	0.40 ± 0.05	1.10 ± 0.09	1.25 ± 0.09	2.57 ± 0.09
Co 6.3–Mo 8.6/Al_2O_3 (Mo first)[a]	1.19	575	0.15 ± 0.05	0.55 ± 0.05		
			0.10 ± 0.05	0		
		300	0.32 ± 0.05	0.56 ± 0.05		
			0.23 ± 0.05	0		
		80	0.43 ± 0.03	0.55 ± 0.03		
			0.30 ± 0.05	0		
Co 5.2–Mo 10.6 (Co first)[a]	0.80	300	0.29 ± 0.05	0.55 ± 0.05		
			0.20 ± 0.05	0		
Co 1–Mo 6/Al_2O_3 (coimp)	0.27	300	0.33 ± 0.03	0.90 ± 0.03		
			1.13 ± 0.03	1.90 ± 0.03		

[a] For these catalysts only the values for the Co_3O_4 component have been listed.

TABLE 3

MES Parameters Obtained from a Computer Analysis (See Text) of the Spectra Recorded at 80 K

Catalyst	Co/Mo	Co_{tet}[a]				Co_{oct}[b]			
		Fe^{3+} component		Fe^{2+} component		Fe^{3+} component		Fe^{2+} component	
		δ (mm s^{-1})	ΔE_Q (mm s^{-1})	δ (mm s^{-1})	ΔE_Q (mm s^{-1})	δ (mm s^{-1})	ΔE_Q (mm s^{-1})	δ (mm s^{-1})	ΔE_Q (mm s^{-1})
Co 0.5–Mo 8.6/Al_2O_3	0.09	0.36	0.68	1.11	2.16	0.45	1.18	1.23	2.78
Co 1.4–Mo 8.6/Al_2O_3	0.27	0.34	0.65	1.10	2.01	0.44	1.17	1.22	2.74
Co 2.8–Mo 8.6/Al_2O_3	0.53[c]	0.36	0.65	1.11	2.09	0.45	1.08	1.20	2.75
Co 4.0–Mo 8.6/Al_2O_3	0.75[c]	0.36	0.70	1.05	2.00	0.45	1.15	1.19	2.62
Co 6.3–Mo 8.6/Al_2O_3	1.19[c]	0.33	0.66	1.08	2.04	0.48	1.16	1.20	2.70

[a] relative uncertainties are ±0.05 mm s^{-1}.

[b] relative uncertainties are ±0.07 mm s^{-1}.

[c] the parameters for the Co_3O_4 component were constrained in accordance with the values for the model compound Co_3O_4.

spectra obtained at 80 K since the different components are best resolved at the low temperature. In the computer fits, the Fe^{2+}/Fe^{3+} area ratio after decay of Co_{tet} (as well as of Co_{oct}) was constrained to be the same for all the catalysts. The high-loading catalysts contain, in addition to Co_{tet} and Co_{oct} as discussed above, also Co_3O_4 and in the fits the Mössbauer parameters of Co_3O_4 were constrained to those of the model compound. Table 3 shows the values obtained for the Mössbauer parameters of Co_{oct} and Co_{tet}. It is seen that the values are in accordance with the expected coordination and also that they do not change significantly from catalyst to catalyst. The individual spectral components as well as the total fit obtained from the computer analysis are shown in Fig. 11 for two of the spectra.

The absolute amount of Co in the different configurations is shown in Fig. 12. It is seen that for catalysts with a Co/Mo ratio below ca. 0.9, Co_{oct} is predominant, whereas at higher Co/Mo ratios Co_3O_4 dominates. For all catalysts Co_{tet} amounts to less than about 20% of all the Co.

c. Sequentially impregnated Co–Mo/Al_2O_3 (Co first) catalysts. A calcined Co/Al_2O_3 catalyst (containing 5.2% Co) was studied by MES before and after subsequent addition of Mo. No significant difference was observed in the MES spectra. This shows that addition of molybdenum does not significantly influence the Co species (i.e., Co_3O_4) already present in the Co/Al_2O_3 catalyst. Studies of catalysts prepared in a similar way by Lo Jacono *et al.* (*33*), Chung and Massoth (*34*), and Breysse *et al.* (*15*) also show that Co_3O_4 formation occurs at a much lower Co loading (or Co/Mo ratio) than in the corresponding Co–Mo/Al_2O_3 catalysts prepared by impregnation with Mo first.

d. Coimpregnated Co–Mo/Al_2O_3 catalysts. Mössbauer spectra of Co1–Mo6/Al_2O_3 (coimp) and Co4–Mo6/Al_2O_3 (coimp) have been discussed earlier (*7, 9, 12*). By analyzing these spectra in detail, it is found

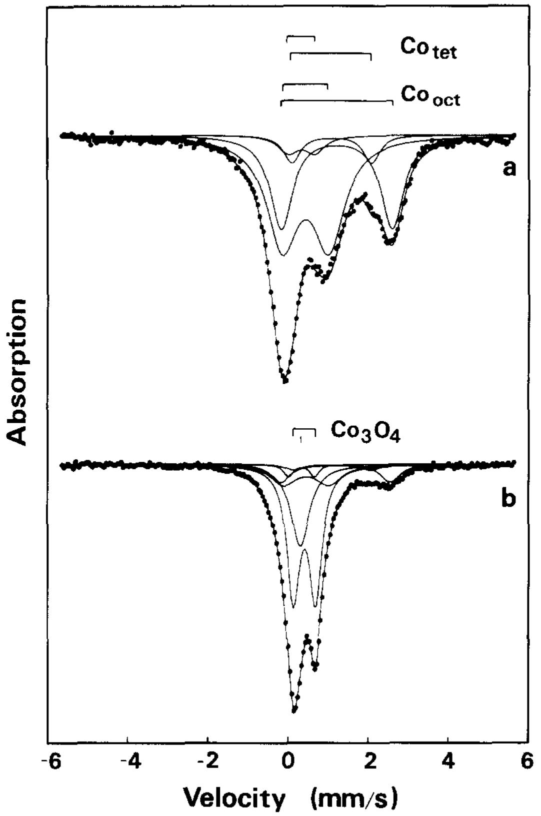

FIG. 11. Examples showing the computer fits of two of the spectra in Fig. 10. The solid lines represent the fits of the individual spectral components as well as the total fit. The spectra were obtained at 80 K; (a) Co/Mo = 0.27, (b) Co/Mo = 1.19.

that in the coimpregnated catalysts, the distribution of Co among the different phases seems to be quite close to that observed for the corresponding Co–Mo/Al$_2$O$_3$ catalysts prepared by impregnation with Mo first.

DISCUSSION

A. Model Compounds

The spectra shown in Figs. 1–4 demonstrate that the model compounds CoO, Co$_3$O$_4$, CoAl$_2$O$_4$, and CoMoO$_4$ give rise to very different Mössbauer spectra. These differences are particularly evident when the temperature dependences of the spectral parameters (Table 1) and of the chemical after-effects are considered. Therefore, MES appears to be a very suitable method for distinguishing between the different cobalt-containing phases which have previously been proposed to be present in calcined Co–Mo/Al$_2$O$_3$ catalysts. The studies of the model compounds also demonstrate how the isomer shift gives information about the coordination of the Co atoms. For atoms of the same coordination, the value of the quadrupole splitting gives further details on the symmetry of the environment. For example, both CoO and CoMoO$_4$ have octahedrally coordinated Co atoms, but very different quadrupole splittings are observed in the spectra. In CoO this splitting is zero, reflecting perfect cubic symmetry, whereas in CoMoO$_4$ nonzero quadrupole splittings are observed reflecting distorted octahedral symmetry.

B. Co/Al$_2$O$_3$ Catalysts

In accordance with the results of previous work (*19, 33–36*), the present results on the calcined Co/Al$_2$O$_3$ catalysts with a high cobalt loading show formation of Co$_3$O$_4$. This results in formation of Co$_9$S$_8$ upon sulfiding and in fact, the Co$_9$S$_8$ appears to originate solely from Co$_3$O$_4$ (see below).

The Mössbauer parameters of the Co 0.25/Al$_2$O$_3$ catalysts show that the Co atoms which interact with the alumina sup-

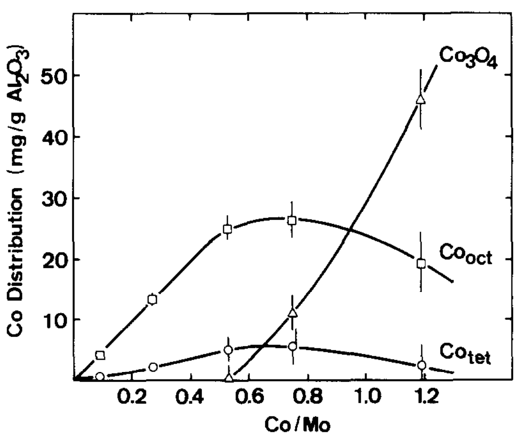

FIG. 12. Absolute amount of cobalt in the three cobalt-containing phases as a function of the Co/Mo ratio.

port are predominantly octahedrally coordinated. Many previous authors (see, e.g., Ref. (*1*)) have proposed that all the cobalt in the alumina is tetrahedrally coordinated as in $CoAl_2O_4$. This conclusion was based mainly on data obtained from DRS, but, as pointed out by Ashley and Mitchell (*35*), this technique is not very sensitive to Co in octahedral coordination and therefore does not exclude that such species are present. Tomlinson *et al.* (*36*) observed relatively high magnetic moments for the Co atoms in a 0.34% Co/Al_2O_3 catalyst, which indicates that the majority of the atoms is octahedrally coordinated. Recent ir experiments (*37*) on a Co $0.26/Al_2O_3$ catalyst, similar to the Co $0.25/Al_2O_3$ catalyst studied here, also support this interpretation.

The ir studies (*37*) also showed that a large fraction of the Co atoms was accessible for NO adsorption indicating that these are located at the surface. The MES results are in accordance with this observation since the spectra of the Co $0.25/Al_2O_3$ catalyst (Fig. 5) were significantly affected by exposure of the calcined catalyst to the sulfiding mixture (and reexposure of this catalyst to air at room temperature (*9*)). The sulfiding does not result in formation of any significant amounts of Co_9S_8 in the low loading catalyst.

Figure 6 shows the amounts of Co in alumina and in Co_3O_4 in the calcined catalysts as a function of Co loading. It is interesting that the amount of Co associated with the alumina lattice seems to go through a maximum and decreases to a very low value at high loadings. Magnetic (*36*), gravimetric (*34*), and NO chemisorption studies (*37*) have also provided results which show a similar behavior. It might be expected that all the Co would be associated with the surface of the alumina until "saturation" was reached and that upon further increase in the Co concentration the excess Co would form Co_3O_4. Obviously, this simple picture does not explain the results, which rather suggest that at high Co concentrations formation of Co_3O_4 crystals is favored at the expense of Co in alumina. More studies are necessary before the behavior is fully understood.

C. *Co–Mo/Al₂O₃ Catalysts: Nature of Co Phases*

The analysis of the MES spectra of the $Co–Mo/Al_2O_3$ catalysts shows that several different cobalt species may be present.

Co_{oct}. In many previous studies of calcined alumina-supported Co–Mo catalysts it has been suggested that the cobalt atoms are tetrahedrally coordinated in the alumina lattice (see, e.g., Refs. (*1, 2, 4, 6*)). Therefore, it is interesting that the present MES results show that in addition to such tetrahedrally coordinated cobalt atoms, cobalt may also have octahedral coordination. In fact, for $Co–Mo/Al_2O_3$ catalysts calcined under the quite mild conditions ($\leq$850 K), usually employed in previous studies, these Co_{oct} atoms are the most abundant form of cobalt.

The present study shows that essentially all Co_{oct} atoms are affected by the sulfiding treatment (see Section D). This result suggests that the majority of the Co_{oct} is located near the surface.

A comparison of the Mössbauer parameters of Co_{oct} and the model compounds shows that Co_{oct} is not due to the presence of a separate phase such as CoO, Co_3O_4, or $CoMoO_4$. The MES lines of Co_{oct} are much broader than those of the above compounds and the Mössbauer parameters and their temperature dependence are also very different.

The possibility that the Co_{oct} component is due to the presence of $CoMoO_4$ or other well-defined Co–Mo phases (e.g., "Mo_4Co" (*38*) or well-defined Co–Mo "bilayers" (*39–42*)) is also inconsistent with the broad MES lines and the Co and Mo EXAFS results (*43, 44*) of the same catalysts. Also, the Mo EXAFS study (*44*) did not show any noticeable difference in the radial distribution function around the Mo atoms in Mo/Al_2O_3 and in $Co–Mo/Al_2O_3$ catalysts. Recent infrared studies (*22, 37,*

TABLE 4

Comparison of NO Uptake and Amount of Co_{oct} in Calcined Co–Mo/Al_2O_3 Catalysts

Catalyst	Co_{NO}[a] (μmol/g cat)	Co_{oct}[b] (μmol/g cat)	$\frac{Co_{oct}}{Co_{NO}}$
0.09	11.8	89	7.5
0.27	30.5	259	8.5
0.44	43.6	386	8.9
1.35	82.8[c]	272	3.3

[a] Number of Co atoms adsorbing NO. The values are calculated from data in Ref. (*23*) taking into account that NO is adsorbed as a dinitrosyl.

[b] Values were obtained from Fig. 11.

[c] Includes also the NO uptake on the Co_3O_4 phase present in the catalyst (*24*).

45) of NO adsorption on Co–Mo/Al_2O_3 catalysts similar to those studied here showed that the surface Co atoms adsorbing NO interact with Mo atoms. Other investigators have also found evidence for Co–Mo interactions (*18, 46–50*). It is seen that the surface Co atoms, which can adsorb NO, are somehow related to Co_{oct} since for all catalysts the number of cobalt atoms adsorbing NO is roughly proportional to the number of Co_{oct} atoms (Table 4). However, the number of Co atoms adsorbing NO is a factor of about 8 smaller than the total number of Co_{oct} atoms. This indicates that the cobalt species termed Co_{oct} may encompass atoms with varying surroundings and that only a small fraction is accessible to adsorption of NO.

The present Mössbauer results show that Co_{oct} has MES parameters which are quite similar to those of the low-loading Co catalyst not containing Mo. Therefore, it seems likely that most of the Co_{oct} atoms are located in the alumina below the Mo layer. The Mo EXAFS results (*44*), which show that the Mo atoms are not notably affected by the presence of Co, are also consistent with such a picture. The interpretation is also in accordance with recent ion scattering spectroscopy (ISS) results (*42, 51*) which show that the Co concentration has its maximum value just below the surface.

Co_{tet}. While only a few studies have suggested the presence of octahedrally coordinated Co, it has been generally accepted that Co may be present in tetrahedral coordination in the alumina lattice. This conclusion has been based mainly on DRS studies which show a triplet band attributed to Co^{2+} in tetrahedral coordination (*33, 35*). The present studies show, however, that these Co_{tet} atoms are only predominant after calcination at high temperatures. This change in coordination of the Co atoms with increasing calcination temperature is also reflected by the color of the catalysts, which is grayish-blue at low calcination temperature, bright blue at intermediate calcination temperature, and deep blue at high calcination temperature.

It is noteworthy that the amount of cobalt which was not affected by the sulfiding (see Fig. 9C) was found to vary with calcination temperature in a way which is quite similar to the amount of tetrahedrally coordinated Co estimated from DRS (*17*). This result confirms that the tetrahedrally coordinated Co species identified by DRS is the same as the Co_{tet} species identified by MES.

The MES results, which show that the Co_{tet} atoms are not notably affected by sulfiding, and the ir results (*37*), which show that these atoms are not accessible for NO adsorption, indicate that the Co_{tet} atoms are predominantly located in subsurface regions of the alumina. The increase in calcination temperature thus seems to result in diffusion of Co from octahedral sites close to the surface to tetrahedral sites in the interior of the alumina.

It has often been assumed that the tetrahedrally coordinated Co is present as $CoAl_2O_4$ in calcined Co–Mo/Al_2O_3 catalysts (see, e.g., Ref. (*5*)). However, the present MES results show that for the catalysts calcined at temperatures up to about 1100 K, the quadrupole splitting for the ferrous doublet is significantly larger than that of $CoAl_2O_4$ (Fig. 9B). This reflects the fact that the symmetry around the Co atoms is different in the two phases. It may there-

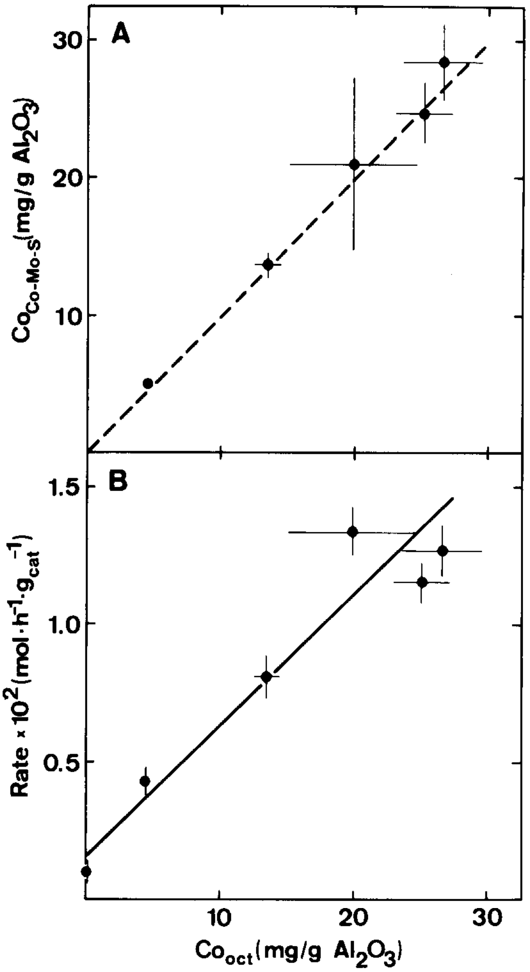

FIG. 13. (A) Absolute amount of cobalt in the Co–Mo–S phase in the sulfided state plotted as a function of the amount of cobalt as Co_{oct} in the calcined state. The dashed line represents a 1 : 1 relation. (B) First-order rate parameter vs the amount of cobalt as Co_{oct}.

fore be reasonable to regard the Co_{tet} species as a solid solution of Co in the defective alumina spinel.

Co_3O_4. In addition to the phases discussed above, Co_3O_4 was found to be present in the catalyst with a high Co loading. The spectral lines of the Co_3O_4 phase are narrow and this indicates that it is well crystallized.

XRD studies of the catalyst with Co/Mo ratios larger than 1.0 confirmed the presence of Co_3O_4. Furthermore, in accordance with the results of Chung and Massoth (*34*), the MES results show that catalysts which were batchwise impregnated with Co first show formation of Co_3O_4 at lower loadings than catalysts which were impregnated with Mo first.

The studies of both the Co/Al_2O_3 and the Co–Mo/Al_2O_3 catalysts show that once the Co_3O_4 formation occurs this phase will be favored at the expense of the other Co phases. As a result, the absolute concentration of Co_{oct} will go through a maximum when the Co concentration is increased. This behavior seems to be a catalytically important feature of Co–Mo/Al_2O_3 catalysts as it appears to be the origin of the variations in the catalytic activity observed for the catalysts after sulfiding. This will be discussed in more detail below.

D. Structural Changes upon Sulfiding. Catalytic Significance of Calcined Precursors

MES studies allow us to follow how the different phases in the calcined catalysts respond to sulfiding. It is seen that there exists a strong "memory" effect. For example, the results for the catalysts calcined at different temperatures (Fig. 9) show that Co_{tet} is not significantly affected by sulfiding, whereas most of the Co_{oct} species appear to be sulfided.

A comparison of the Co phase distribution of the calcined Co–Mo/Al_2O_3 catalysts (Fig. 12) with the phase distribution of the same catalysts after sulfiding (Fig. 6 in Ref. (*13*)) shows that there exists a correlation between the amount of Co present as Co_{oct} in the calcined state and the amount of Co present as Co–Mo–S after sulfiding. The plot of the amount of Co in Co–Mo–S as a function of the amount of Co_{oct}, shown in Fig. 13A, indicates that essentially all the Co_{oct} is sulfided to Co–Mo–S. In fact, Co_{oct} seems to be the only precursor to Co–Mo–S.

However, it should be noted that this relationship is probably only valid for alumina-supported catalysts since other types

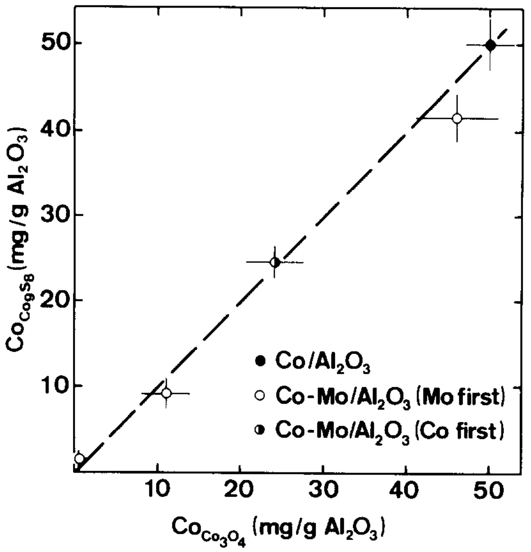

FIG. 14. Absolute amount of cobalt as Co_9S_8 in the sulfided catalysts plotted as a function of the amount of cobalt as Co_3O_4 in the calcined state. The dashed line represents a 1 : 1 relation.

of Co–Mo catalysts (e.g., unsupported (*6, 7, 12, 14, 16*), silica-supported (*8*), and carbon-supported (*8, 15*) catalysts) may have other types of Co precursors to the Co–Mo–S phase. The reason why Co_{oct} is a precursor for the formation of Co–Mo–S in alumina-supported Co–Mo catalysts is probably related to its location close to the Mo atoms.

By comparing the results in Fig. 12 with those given in Ref. (*13*) it is found that the amount of Co_{tet} in the calcined catalysts is very similar to the amount of Co present in the alumina after sulfiding. This result shows that Co_{tet} is not affected to any significant extent by the sulfiding treatment used presently. However, at higher temperatures Co_{tet} may also be sulfided.

It is found that Co_3O_4 is sulfided, but the resulting phase is Co_9S_8 and not Co–Mo–S. This can be concluded from Fig. 14 which shows that the amount of Co in the form of Co_9S_8 after sulfiding is equal to the amount of Co_3O_4 in the calcined state for all the Co/Al_2O_3 and Co–Mo/Al_2O_3 catalysts studied here.

Recent results have shown that the promotion of the HDS activity is related to the Co atoms in the Co–Mo–S phase (*6, 11, 13–17*). From a catalytic point of view, the Co_{oct} species is consequently the most important Co phase in calcined Co–Mo/Al_2O_3 catalysts since this Co species appears to be the only precursor for the Co–Mo–S phase. As shown in Fig. 13B the increase in the HDS activity is in fact proportional to the amount of Co_{oct} present before sulfiding. (The observation that the line in Fig. 13B does not pass through the origin simply expresses the fact that unpromoted catalysts also have some catalytic activity.) One goal in the preparation of catalysts with high HDS activity should therefore be to optimize the concentration of Co_{oct} and to minimize the amount of Co present in other forms.

On the basis of the present results it is possible to explain why different catalysts with the same total Co loading have been reported to exhibit quite different catalytic activities, and why different investigators find the optimum in catalytic activity to occur at different Co/Mo ratios. For example, catalysts prepared by impregnation with Co first in relatively large amounts have been observed to have a low promotional effect of Co (*19, 20*). This is expected because such a preparation favors the formation of Co_3O_4 which is sulfided to Co_9S_8 and not to Co–Mo–S.

The HDS activity of Co–Mo/Al_2O_3 usually goes through a maximum when the Co loading (or Co/Mo ratio) is increased. In the previous study of the catalysts in the sulfided state (*13*) it was not possible to establish with certainty whether the decrease in the activity observed at high Co/Mo ratios is associated with a reduction in the amount of Co present as Co–Mo–S or due to other effects such as, e.g., a covering (poisoning) of the Co–Mo–S phase by Co_9S_8. However, the decrease in the amount of Co_{oct}, which seems to occur at high Co/Mo ratios, suggests that the decline in the activity is due to a decrease in the concentration of Co atoms present in the form of Co–Mo–S.

CONCLUSIONS

The present experiments demonstrate the usefulness of the Mössbauer emission technique for providing qualitative as well as quantitative information about Co atoms in calcined Co–Mo/Al_2O_3 catalysts.

From a structural point of view the results show that typical calcined Co–Mo/Al_2O_3 catalysts have a major fraction of the Co atoms present in octahedral-like coordination (Co_{oct}) near the alumina surface. This has not been generally accepted in the past. However, in accordance with many previous investigations the present results also show that Co may be found in tetrahedral sites inside the alumina (in a form different from $CoAl_2O_4$) or as a separate Co_3O_4 phase.

The presence of the Co_{oct} species is seen to have important consequences for the catalytic activity since it is observed that Co_{oct} transforms into the catalytically active Co–Mo–S phase upon sulfiding. The other Co phases observed in the calcined catalysts were found not to be precursors for Co–Mo–S. As a result, the observed changes in the HDS activity could be related to the variations in the abundance of Co_{oct} for all the catalysts studied.

ACKNOWLEDGMENT

The technical assistance of J. W. Ørnbo during several phases of this work is gratefully acknowledged.

REFERENCES

1. Schuit, G. C. A., and Gates, B. C., *AIChE J.* **19,** 417 (1973).
2. Massoth, F. E., *in* "Advances in Catalysis" (D. D. Eley, H. Pines, and P. B. Weiz, Eds.), Vol. 27, p. 265. Academic Press, New York, 1978.
3. Grange, P., *Catal. Rev.—Sci. Eng.* **21,** 135 (1980).
4. Ratnasamy, P., and Sivasanker, S., *Catal. Rev.–Sci. Eng.* **22,** 401 (1980).
5. Delmon, B., *in* "Proceedings of the Climax Third International Conference on Chemistry and Uses of Molybdenum" (H. F. Barry, and P. C. H. Mitchell, Eds.), p. 73. Climax Molybdenum Co., Ann Arbor, Mich., 1979.
6. Topsøe, H., Clausen, B. S., Candia, R., Wivel, C., and Mørup, S., *Bull. Soc. Chim. Belg.* **90,** 1189 (1981).
7. Clausen, B. S., Mørup, S., Topsøe, H., and Candia, R., *J. Phys. Colloq.* **37,** C6-249 (1976).
8. Topsøe, H., Clausen, B. S., Burriesci, N., Candia, R., and Mørup, S., *in* "Preparation of Catalysts II" (B. Delmon, P. Grange, P. Jacobs, and G. Poncelet, Eds.). Elsevier, Amsterdam, 1979.
9. Clausen, B. S., Ph.D. Dissertation, Technical University of Denmark (1979).
10. Mørup, S., Clausen, B. S., and Topsøe, H., *J. Phys. Colloq.* **40,** C2-88 (1979).
11. Wivel, C., M.Sc. Dissertation, University of Copenhagen (1980).
12. Topsøe, H., Clausen, B. S., Candia, R., Wivel, C., and Mørup, S., *J. Catal.* **68,** 433 (1981).
13. Wivel, C., Candia, R., Clausen, B. S., Mørup, S., and Topsøe, H., *J. Catal.* **68,** 453 (1981).
14. Candia, R., Clausen, B. S., and Topsøe, H., *Bull. Soc. Chim. Belg.* **90,** 1225 (1981).
15. Breysse, M., Bennett, B. A., Chadwick, D., and Vrinat, M., *Bull. Soc. Chim. Belg.* **90,** 1271 (1981).
16. Candia, R., Clausen, B. S., and Topsøe, H., *J. Catal.* **77,** 564 (1982).
17. Candia, R., Topsøe, N.-Y., Clausen, B. S., Wivel, C., Nevald, R., Mørup, S., and Topsøe, H., *in* "Proceedings of the Fourth Climax International Conference on Chemistry, and Uses of Molybdenum" (H. F. Barry and P. C. H. Mitchell, Eds.), p. 374. Climax Molybdenum Co., Ann Arbor, Mich., 1983.
18. Richardson, J. T., *Ind. Eng. Chem. Fundam.* **3,** 154 (1964).
19. Declerck-Grimee, R. I., Canesson, P., Friedman, R. M., and Fripiat, J. J., *J. Phys. Chem.* **82,** 889 (1978).
20. Massoth, F. E., and Chung, K. S., *in* "Proceedings, 7th International Congress on Catalysis, Tokyo, 1980," p. 629. Elsevier, Amsterdam, 1981.
21. Chiplunker, P., Martinez, N. P., and Mitchell, P. C. H., *Bull. Soc. Chim. Belg.* **90,** 1319 (1981).
22. Topsøe, N.-Y., and Topsøe, H., *J. Catal.* **77,** 293 (1982).
23. Wertheim, G. K., *Phys. Rev.* **124,** 764 (1961).
24. Son, C. J., and Mullen, J. G., *Phys. Rev.* **B14,** 2761 (1976).
25. Spencer, C. D., and Schroeer, D., *Phys. Rev.* **B9,** 3658 (1974).
26. Angeletti, C., Pepe, F., and Porta, P., *J. Chem. Soc. Faraday Trans. I* **73,** 1972 (1977).
27. Clausen, B. S., Topsøe, H., Villadsen, J., and Mørup, S., *in* "Proceedings of the International Conference on Mössbauer Spectroscopy, Bucharest, Romania, 1977" (D. Barb and D. Tarina, Eds.), Vol. 1, p. 155.
28. Smith, G. W., and Ibers, J. A., *Acta Cryst.* **19,** 269 (1965).
29. Clausen, B. S., Topsøe, H., Villadsen, J., Mørup,

S., and Candia, R., *in* "Proceedings of the International Conference on Mössbauer Spectroscopy, Bucharest, Romania, 1977" (D. Barb and D. Tarina, Eds.), Vol. 1, p. 177.

30. Window, B., *J. Phys. E: Sci. Instrum.* **4,** 401 (1971).

31. Hesse, H., and Rübartsch, A., *J. Phys. E: Sci. Instrum.* **7,** 526 (1974).

32. Wivel, C., and Mørup, S., *J. Phys. E: Sci. Instrum.* **14,** 605 (1981).

33. Lo Jacono, M., Cimino, A., and Schuit, G. C. A., *Gazz. Chim. Ital.* **103,** 1281 (1973).

34. Chung, K. S., and Massoth, F. E., *J. Catal.* **64,** 320, 332 (1980).

35. Ashley, J. H., and Mitchell, P. C. H., *J. Chem. Soc. A* 2821 (1968).

36. Tomlinson, J. R., Keeling, R. O., Rymer, G. T., and Bridges, J. M., *in* "Actes 2me Congr. Int. Catal. Paris, 1960," p. 1831. Editions Technip, Paris, 1961.

37. Topsøe, N.-Y., and Topsøe, H., *J. Catal.* **75,** 354 (1982).

38. Grimblot, J., and Bonnelle, J. P., *J. Electron. Spectrosc. Relat. Phenom.* **9,** 449 (1976).

39. Apecetche, M. A., and Delmon, B., *React. Kinet. Catal. Lett.* **12,** 385 (1979).

40. Gajardo, P., Grange, P., and Delmon, B., *J. Catal.* **63,** 201 (1980).

41. Okamoto, Y., Imanaka, T., and Terinishi, S., *J. Catal.* **65,** 448 (1980).

42. Delannay, F., Haeussler, E. N., and Delmon, B., *J. Catal.* **66,** 469 (1980).

43. Clausen, B. S., Lengeler, B., Candia, R., Als-Nielsen, J., and Topsøe, H., *Bull. Soc. Chim. Belg.* **90,** 1249 (1981).

44. Clausen, B. S., Topsøe, H., Candia, R., Villadsen, J., Lengeler, B., Als-Nielsen, J., and Christensen, F., *J. Phys. Chem.* **85,** 3868 (1981).

45. Topsøe, N.-Y., and Topsøe, H., *Bull. Soc. Chim. Belg.* **90,** 1311 (1981).

46. Medema, J., van Stam, C., de Beer, V. H. J., Konings, A. J. A., and Koningsberger, D. C., *J. Catal.* **53,** 386 (1978).

47. Cheng, C. P., and Schrader, G. L., *J. Catal.* **60,** 276 (1979).

48. Moné, R., and Moscou. L., *Amer. Chem. Soc. Ser.* **20,** 150 (1975).

49. Ratnasamy, P., and Knözinger, H., *J. Catal.* **54,** 155 (1978).

50. Topsøe, N.-Y., *J. Catal.* **64,** 235 (1980).

51. Chin, R. L., and Hercules, D. M., *J. Phys. Chem.* **86,** 3079 (1982).